Supplemental material

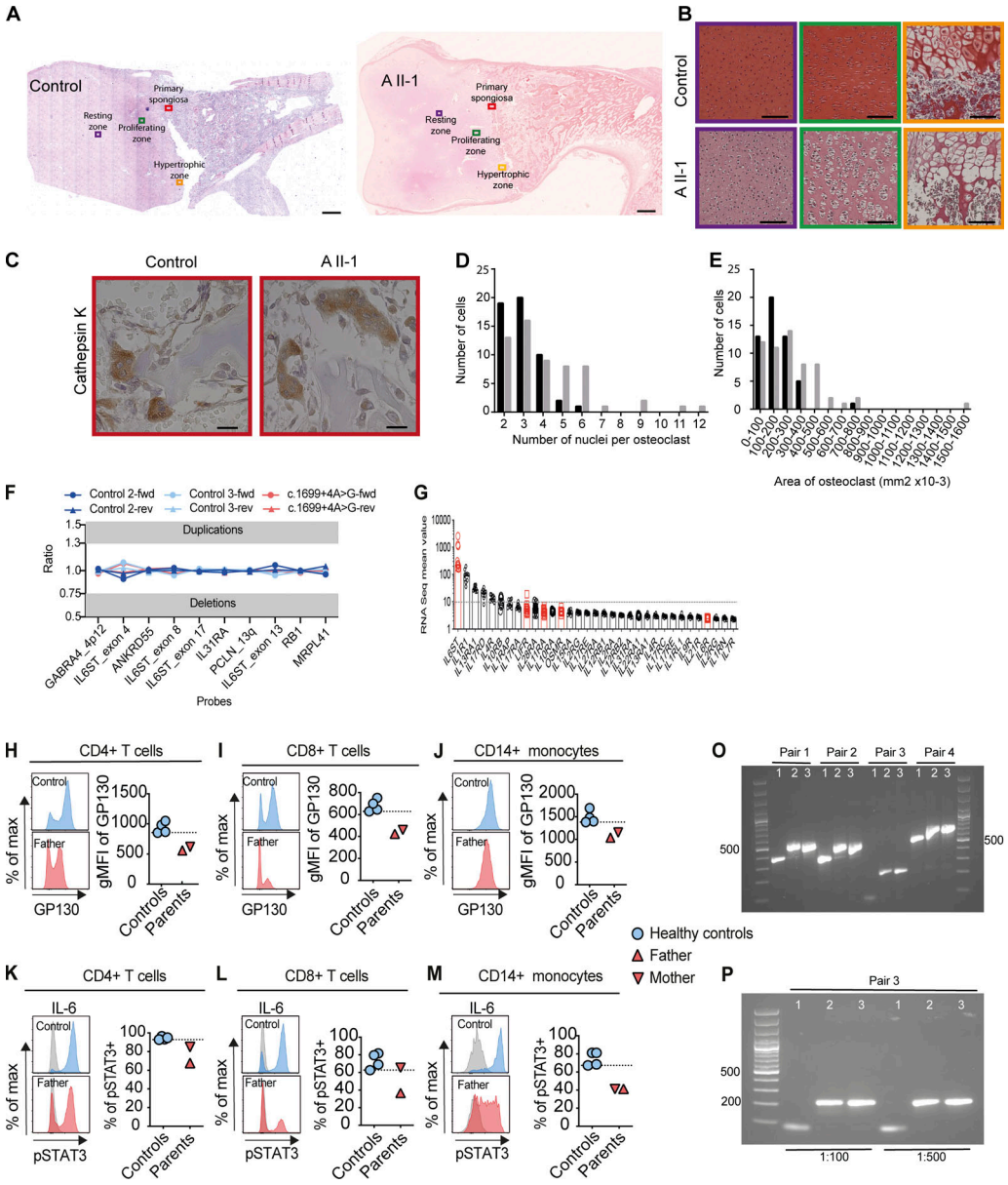

Figure S1. **Bone phenotype, MLPA analysis of the *IL6ST* gene, RNA-seq expression data of multiple cytokine receptor units in control amniocytes, the parental analysis of GP130 and pSTAT3 response, and PCR analysis. (A)** H&E staining of femur bones from affected patient A-II-1 and an age-matched control. Several anatomic regions are labeled and color-coordinated, for guidance in the other panels. Scale bar indicates 1 mm. **(B)** Growth plate zones following safranin O/fast green (SOFG) staining show resting (left), proliferative (middle), and hypertrophic (right panel) zones. Scale bar indicates 50 µm. **(C)** Multinuclear osteoclasts in the primary spongiosa were visualized by immunostaining for Cathepsin K and counterstaining with hematoxylin. Scale bar indicates 20 µm. **(D)** Quantification of the number of nuclei in cathepsin K–positive cells, with only cells containing two or more nuclei counted. **(E)** Quantification of the size of cathepsin K–positive cells containing two or more nuclei. **(C–E)** Six visual fields analyzed with three images from each side of the bone; black bars indicate control; gray bars indicate patient A-II-1. Note that colored boxes surrounding images in B and C correspond to regions indicated in A. **(F)** Ratio for each probe (deletions would cause a ratio of <0.75 and duplications of >1.3). Exons 4, 8, 13, and 17 in *IL6ST* and genes upstream and downstream of *IL6ST* (*ANKRD55* and *IL31RA*) were investigated. **(G)** RNA-seq expression of multiple cytokine receptor units in control amniocytes. In case of multiple RNA-Seq Probe Set IDs of each receptor, the one with highest expression was shown. Blue lines represent the median of n = 11 individual amniocyte samples. GP130-dependent cytokine receptors are shown in red. Each dot represents one individual sample, data taken from Kang et al. (2015). **(H–J)** GP130 surface expression in ex vivo $CD3^+CD4^+$, $CD3^+CD8^+$, and $CD14^+$ cells gated from peripheral blood mononuclear cells of heterozygous parents compared with four healthy donors. Representative histograms of one control and the father (left) and geometric mean florescence intensity (gMFI; right) are shown. **(K–M)** Response of pSTAT3 in heterozygous parents after stimulation with IL-6 (100 ng/ml for 15 min) compared with four healthy controls (gray, unstimulated; blue and red, stimulated). Representative histograms are shown on the left. **(H–M)** Blue, controls; red, father (upper triangle) and mother (lower triangle). Dashed line indicates the lowest value from the healthy controls. **(O–P)** Agarose gels for RT-PCR and nested PCR using four primer pairs (pair 1, exon 11 and boundary of exons 14–15; pair 2, exons 12–16; pair 3, exons 12–14; pair 4 exons 11–16). 1, amplicon from cDNA from EBV-LCLs of patient C-II-3 with c.1699+4A>G variant; 2–3, control EBV-LCLs, 100-bp ladder on the side of each gel. **(P)** Nested PCR using amplicons from exons 12–14 with primer pair 3. Amplicon of expected 218-bp size in control samples versus amplicon of ∼70-bp in patient sample confirming skipping of exon 13. 1:100 and 1:500 indicate dilution ratio for the RT-PCR products.

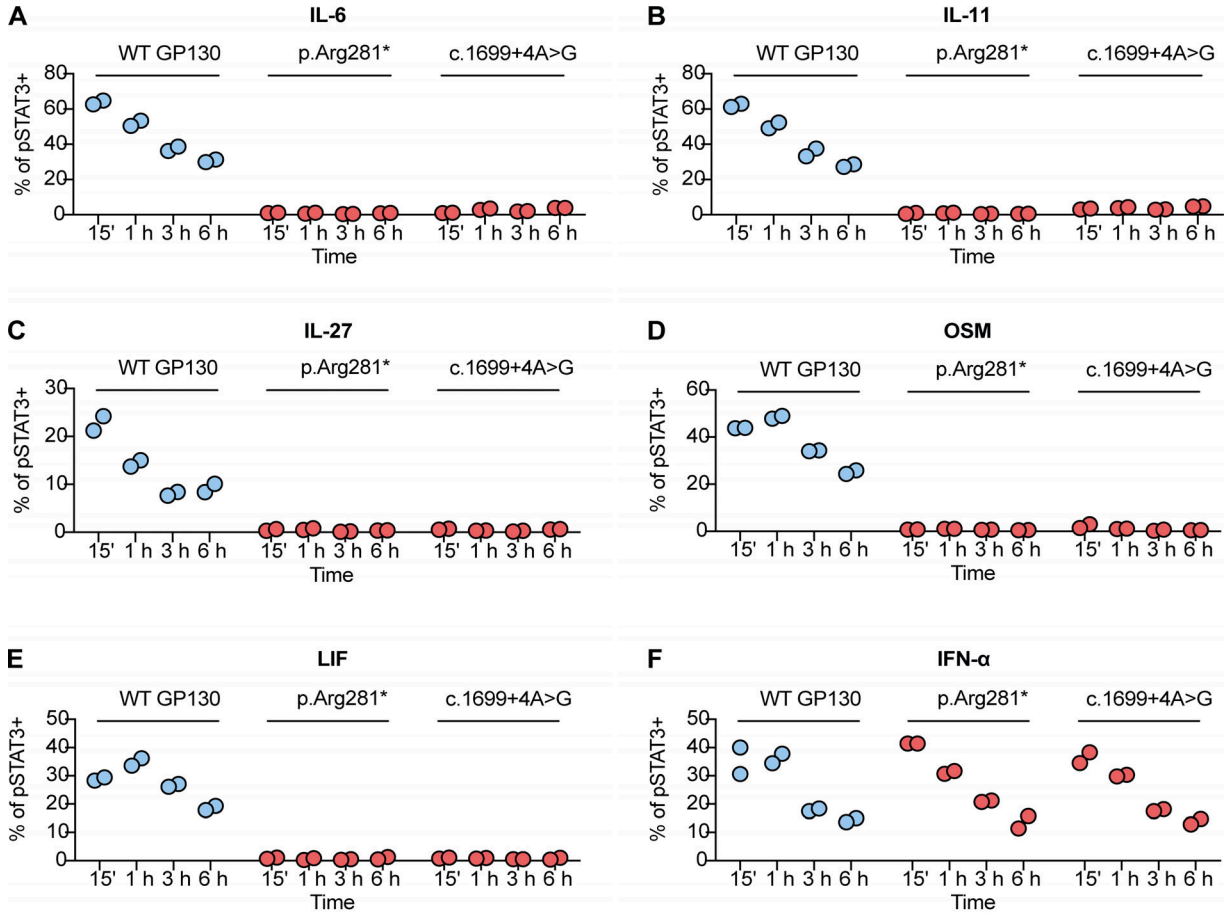

G

Cytokine signaling defects		Symptoms
IL-11/IL-11RA	IL-11R deficiency	Craniosynostosis, delayed teeth
IL-6/IL-6RA	IL-6R deficiency Anti-6R treatment IL-6 autoantibodies	Delayed acute phase response, infection susceptibility, eczematous dermatitis, Hyper-IgE
IL-27/WSX-1	Not known in human	
OSM/OSMR	Anti-OSM treatment	Haematopoietic - thrombocytopenia
LIF/LIFR	LIFR deficiency	Stüve-Wiedemann syndrome Musculoskeletal system: short stature, bowing of extremities principally affecting the lower limbs, hypoplastic midface, osteopenia with fractures later in life, congenital contractures. Respiratory system: respiratory distress/ apnea exacerbated by swallowing difficulties leading to aspiration pneumonia. Nervous system: delayed motor development, muscular hypotonia, dysautonomia with temperature instability leading to episodes of hyperthermia, absent corneal and patellar reflexes. Kidney malformations.

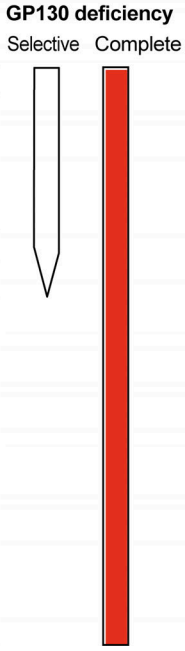

Figure S2. **The complete loss of GP130-dependent IL-6, IL-11, IL-27, OSM, and LIF signaling in p.Arg281* and c.1699+4A>G variant is not due to delayed kinetics; and a schematic summary of GP130 deficiency, the relationship between loss of cytokine signaling and clinical symptoms. (A–F)** Response of pSTAT3 in c.1699+4A>G transfected GP130-deficient HEK293 after stimulations with IL-6, IL-11, IL-27, OSM, LIF, and IFN-α stimulation (all 100 ng/ml) over a time course covering 15 min, 1 h, 3 h, and 6 h. For assessment of IL-6 and IL-11 signaling, cells were cotransfected with plasmids encoding IL-6Rα and IL-11Rα, respectively. Successfully transfected cells were gated based on GFP expression. Quantification is based on individual independent experiments per cytokine, with duplicates per experiment. **(G)** A schematic summary of GP130 deficiency and the relationship between loss of cytokine signaling and clinical symptoms. The symptoms described in red were noticed in our patients.

Table S1 is provided online as a separate Word file and lists rare sequence variants identified using whole-genome variant analysis in family A (quadro) and whole exome variant analysis in families B and C (trios).